Supplementary Information for

The Potential Role of H_2S in The Anti-infective Function of Antimicrobial Peptides

Xu Wang[1,2,3,4], Shuangyu Li[1,4,5], Wenzhuang Shi[1,4], Beiru Xue[4], Xu Wang[4], Miao Liu[4], Binjuan Lu[4], Zhouye Xu[4], Ye Gao[4], Jiachang Liu[2,3], Xingyue Ji[4], Jia-Tang Li[2,3,5*], Yipeng Wang[1,4,5*]

[1] Key Laboratory of Coastal Zone Biology and Bioresource Utilization, Yantai Institute of Coastal Zone Research, Chinese Academy of Sciences, Yantai, Shandong 264003, China.
[2] Mountain Ecological Restoration and Biodiversity Conservation Key Laboratory of Sichuan Province, Chengdu Institute of Biology, Chinese Academy of Sciences, Chengdu 610213, China
[3] China-Croatia Belt and Road Joint Laboratory on Biodiversity and Ecosystem Services, Chengdu Institute of Biology Chinese Academy of Sciences Chengdu 610213, China.
[4] College of Pharmaceutical Sciences, Soochow University, Suzhou, Jiangsu 215123, China.
[5] University of Chinese Academy of Sciences; Beijing 100049, China.

*Correspondence and material requests should be addressed to J.T.L. (lijt@cib.ac.cn) or Y.P.W. (email: ypwang@yic.ac.cn)

List of Supplementary Information

Table S1 to Table S7

Fig. S1 to Fig. S28

Supporting Information Text

Table S1. Bacterial strains used in this study.

	Bacteria	
	Name	**Standard**
Gram-positive		
	Enterococcus faecalis	ATCC29212
	Bacillus cereus	CMCC63301
	Clostridium perfringens	/
	Bacillus subtilis	CMCC63501
	Staphylococcus aureus	CMCC26003
	Methicillin-resistant	ATCC43300
	Staphylococcus aureus (MRSA)	
	Staphylococcus epidermidis	/
Gram-negative		
	Acinetobacter baumannii 2	/
	Acinetobacter baumannii 6	/
	Acinetobacter baumannii 11	/
	Acinetobacter baumannii 16	/
	Acinetobacter baumannii 19606	/
	Vibrio alginolyticus	/
	Vibrio vulnificus 1755	/
	Shigella flexneri	ATCC12022
	Vibrio harveyi 0593	/
	Escherichia coli	ATCC25922
	Escherichia coli	CMCC44102
	Pseudomonas aeruginosa	CMCC10104

"/": clinically isolated strain from Second Affiliated Hospital of Soochow University

Table S2. Detail information of antimicrobial peptides used in this study

Peptides	Sequence	Length	Net charge	Theoretical pI	Mw	Source
LL-37	LLGDFFRKSKEKIGKEFKRIVQRIKDFLRNLVPRTES	37	+6	10.61	4493.40	*Homo sapiens*
CRAMP	GLLRKGGEKIGEKLKKIGQKIKNFFQKLVPQPE	33	+6	10.22	3878.80	*Mus musculus*
Brevinin-1AW6	LLPLLAGLAAKLVPTVLCKISRRC	24	+4	10.11	2547.20	*Amolops wuyiensis*
CATHPb1	KRFKKFFRKIKKGFRKIFKKTKIFIGGTIPI	31	+13	12.33	3800.80	*Python bivittatu*
CATHPb4	TRSRWRRFIRGAGRFARRYGWRIALGLVG	29	+9	12.54	3492.11	*Python bivittatu*
Hc-CATH	KFFKRLLKSVRRAVKKFRKKPRLIGLSTLL	30	+12	12.61	3628.50	*Hydrophis cyanocinctus*
GoatCATH1	RITKQPWAPPQAARICQFVLIRVCR	25	+5	11.54	2591.59	*Capra hircus*
GoatMAP34-B	GLFGRLRDSLRRGGQKILEKVERIGDRIKDIFRG	34	+5	11.29	3955.63	*Capra hircus*
Cm-CATH2	RRSRFGRFFKKVRKQLGRVLRHSRITVGGRMRF	33	+13	12.96	4089.90	*Chelonia mydas*
ScrLL-37	GLKLRFEFSKIKGEFLKTPEVRFRDIKLKDNRISVQR	37	+6	10.61	4493.40	/

Table S3. The minimum inhibitory concentrations (MICs) of LL-37/CRAMP and polymyxin B against the screened bacteria

Bacteria	Peptides				Antibiotic	
	CRAMP		LL-37		Polymyxin B	
	(μM)	(μg/mL)	(μM)	(μg/mL)	(μM)	(μg/mL)
Gram-positive						
Enterococcus faecalis ATCC29212	38.7	150.0	33.4	150.0	4.0	4.7
Bacillus cereus CMCC63301	19.4	75.0	33.4	150.0	1.9	2.3
Clostridium perfringens	19.4	75.0	33.4	150.0	4.0	4.7
Gram-negative						
Escherichia coli CMCC44102	19.4	75.0	33.4	150.0	4.0	4.7
Vibrio alginolyticus	19.4	75.0	16.7	75.0	1.9	2.3
Vibrio vulnificus 1755	19.4	75.0	33.4	150.0	4.0	4.7
Shigella flexneri ATCC12022	19.4	75.0	33.4	150.0	4.0	4.7
Vibrio harveyi 0593	38.7	150.0	33.4	150.0	1.9	2.3
GM[a]	43.6	93.8	31.3	140.6	3.21	3.8

a. The geometric mean of MICs from eight bacterial strains

Table S4. The minimum inhibitory concentration (MIC) of ScrLL-37 against the screened bacteria.

	Peptides
Bacteria	ScrLL-37
Gram-positive	
Enterococcus faecalis ATCC29212	ND
Bacillus cereus CMCC63301	ND
Clostridium perfringens	ND
Gram-negative	
Escherichia coli CMCC44102	ND
Vibrio alginolyticus	ND
Vibrio vulnificus 1755	ND
Shigella flexneri ATCC12022	ND
Vibrio harveyi 0593	ND

ND: Not detected at the concentration of 200 μg/mL.

Table S5. The minimum inhibitory concentration (MIC) of 7b and BT against *Clostridium perfringens* and *Escherichia coli* CMCC44102.

	Compound	
Bacteria	7b	BT
Clostridium perfringens	ND	ND
Escherichia coli CMCC44102	ND	ND

7b: H_2S scavenger; BT: ROS scavenger ND: Not detected at the concentration of 200 μg/mL.

Table S6. The minimum inhibitory concentration (MIC) of PAG/AOAA/Asp against *Clostridium perfringens* and *Escherichia coli* CMCC44102.

	Compound					
Bacteria	PAG		AOAA		Asp	
Clostridium perfringens	ND	ND	ND	ND	ND	ND
Escherichia coli CMCC44102	ND	ND	ND	ND	ND	ND

ND: Not detected at the concentration of 200 μg/mL. DL-propargylglycine (PAG), aminooxyacetate (AOAA), aspartate (Asp).

Table S7. Comparative analysis of mapped reads and the reference genome.

Sample name	C1	C2	C3	L1	L2	L3
Total reads	20287956	18396152	22552498	19993534	19419910	19711080
Total mapped	19463104	17587779	21546138	19170667	18682979	18852619
	(95.93%)	(95.61%)	(95.54%)	(95.88%)	(96.21%)	(95.64%)
Mutiple mapped	2521503	1494183	1718393	1325911	1798376	1607768
	(12.43%)	(8.12%)	(7.62%)	(6.63%)	(9.26%)	(8.16%)
Uniquely mapped	16941601	16093596	19827745	17844756	16884603	17244851
	(83.51%)	(87.48%)	(87.92%)	(89.25%)	(86.94%)	(87.49%)
Read-1 mapped	8474322	8048567	9916129	8923512	8447288	8625128
	(41.77%)	(43.75%)	(43.97%)	(44.63%)	(43.50%)	(43.76%)
Read-2 mapped	8467279	8045029	9911616	8921244	8437315	8619723
	(41.74%)	(43.73%)	(43.95%)	(44.62%)	(43.45%)	(43.73%)
Reads map to '+'	8470562	8046764	9913814	8922662	8442805	8622379
	(41.75%)	(43.74%)	(43.96%)	(44.63%)	(43.47%)	(43.74%)
Reads map to '-'	8471039	8046832	9913931	8922094	8441798	8622472
	(41.75%)	(43.74%)	(43.96%)	(44.62%)	(43.47%)	(43.74%)
Non-splice reads	16941601	16093596	19827745	17844756	16884603	17244851
	(83.51%)	(87.48%)	(87.92%)	(89.25%)	(86.94%)	(87.49%)
Reads mapped	16363844	15676136	19253526	17330780	16388170	16708408
in proper pairs	(80.66%)	(85.21%)	(85.37%)	(86.68%)	(84.39%)	(84.77%)

C1, C2, C3 stand for the three untreated bacteria，L1, L2, L3 stand for the three LL-37 treated bacteria.

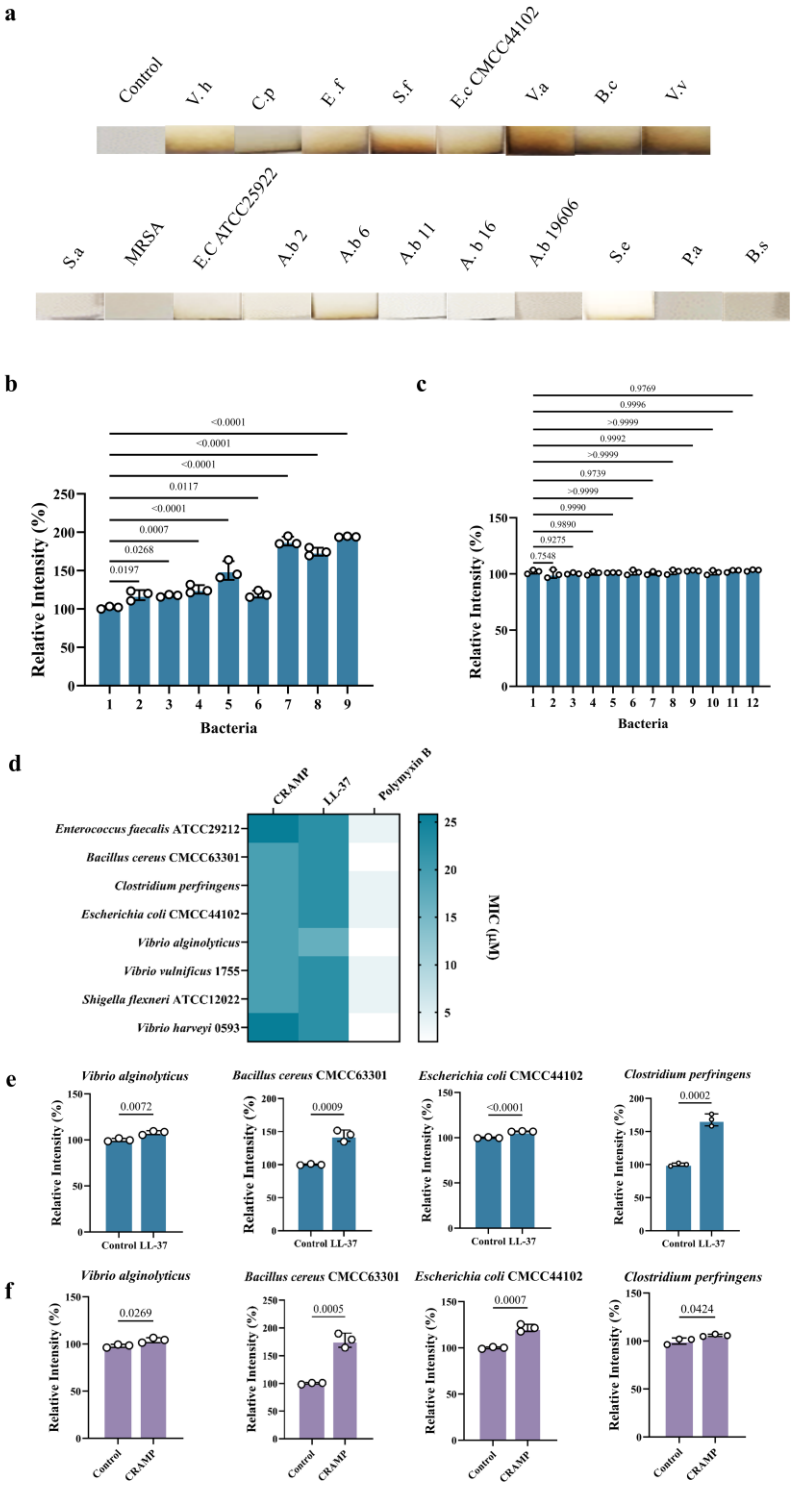

Fig. S1 (**a**) Results of representative Pb-acetate soaked paper strips of 19 strains. V.h: *Vibrio harveyi*, C.p: *Clostridium perfringens*, E.f: *Enterococcus faecalis*, ATCC29212, S.f: *Shigella flexneri* ATCC12022, E.c: *Escherichia coli*, V.a: *Vibrio alginolyticus*, B.c: *Bacillus cereus* CMCC63301, V.v: *Vibrio vulnificus* 1755, S.a: *Staphylococcus aureus*, MRSA: *Methicillin-resistant Staphylococcus aureus*, A.b: *Acinetobacter*

baumannii, S.e: *Staphylococcus epidermidis*, P.a: *Pseudomonas aeruginosa* CMCC10104, B.s: *Bacillus subtilis*. (**b**) Quantitative results of brown stains of PbS on representative Pb-acetate–soaked paper strips from the obvious H_2S-producing bacteria using ImageJ software. 1: Control, 2: *Vibrio harveyi*, 3: *Clostridium perfringens*, 4: *Enterococcus faecalis* ATCC29212, 5: *Shigella flexneri* ATCC12022, 6: *Escherichia coli* CMCC44102, 7: *Vibrio alginolyticus*, 8: *Bacillus cereus* CMCC63301, 9: *Vibrio vulnificus* 1755. (**c**) Quantitative results of brown stains of PbS on representative Pb-acetate–soaked paper strips from the inconspicuous H_2S-producing bacteria using ImageJ software. 1: Control, 2: *Staphylococcus aureus*, 3: *Methicillinresistant Staphylococcus aureus*, 4: *Escherichia coli* ATCC25922, 5: *Acinetobacter baumannii* 2, 6: *Acinetobacter baumannii* 6, 7: *Acinetobacter baumannii* 11, 8: *Acinetobacter baumannii* 16, 9: *Acinetobacter baumannii* 19606, 10: *Staphylococcus epidermidis*, 11: *Pseudomonas aeruginosa* CMCC10104, 12: *Bacillus subtilis*. (**d**) Antimicrobial activity of CRAMP/LL-37 and polymyxin B against the screened bacterial strains; Heat maps show MIC (μM) values. Quantitative results of brown stains of PbS on representative Pb-acetate–soaked paper strips using imageJ software. (**e**-**f**) Lead acetate paper results shows four bacteria were treated with LL-37 and CRAMP, respectively. Numbers indicates relative H_2S content related to the wild-type (WT) bacteria. The results are expressed as mean ± S.D. n = 3 biological replicates. One-way ANOVA followed by Tukey's post hoc analysis. Source data are provided as a Source Data file.

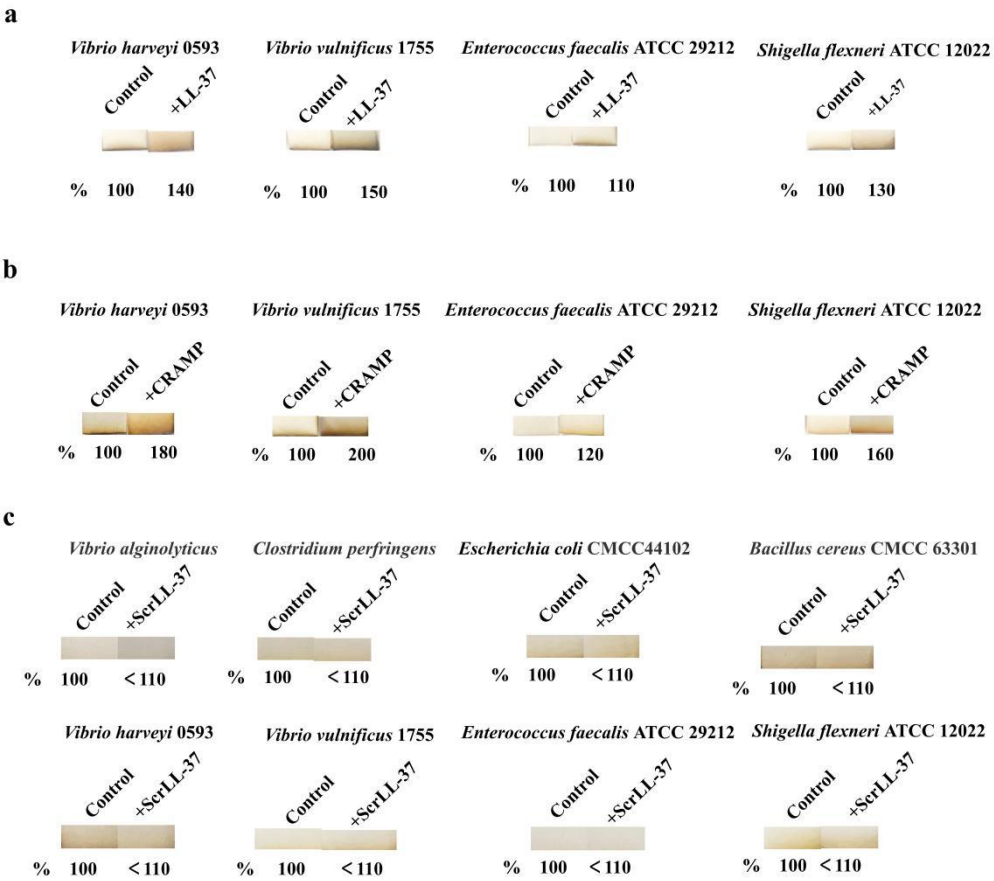

Fig. S2 Representative Pb-acetate soaked paper strips show a brown stain of PbS with quantitative numbers (bottom) as a result of the reaction with gaseous H_2S exiting liquid bacterial cultures (*Vibrio harveyi* 0593, *Vibrio vulnificus* 1755, *Vibrio vulnificus* 1755 and *Shigella flexneri* ATCC12022) promoted by LL-37 (**a**) and CRAMP (**b**). (**c**) Representative Pb-acetate soaked paper strips show a brown stain of PbS with quantitative numbers (bottom). H_2S production on the screened bacteria (*Vibrio alginolyticus*, *Clostridium perfringens*, *Escherichia coli* CMCC44102, *Bacillus cereus* CMCC 63301, *Vibrio harveyi* 0593, *Vibrio vulnificus* 1755, *Vibrio vulnificus* 1755 and *Shigella flexneri* ATCC 12022) treated with ScrLL-37.

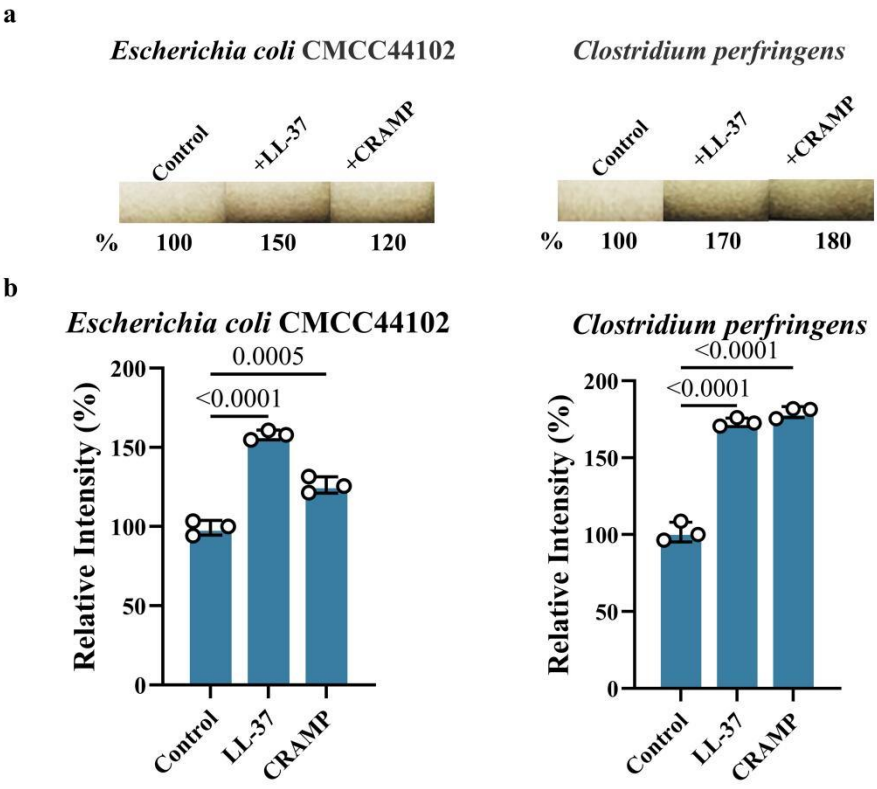

Fig. S3 (**a**) Representative Pb-acetate soaked paper strips show a brown stain of PbS with quantitative values (bottom) related to the wild-type (WT) bacteria cultured for 24 hours as a result of the reaction with gaseous H_2S exiting liquid bacterial cultures (*Escherichia coli* CMCC44102 and *Clostridium perfringens*) promoted by LL-37 and CRAMP. (**b**) Quantitative results of brown stains of PbS on representative Pb-acetate–soaked paper strips using ImageJ software. Lead acetate paper results show *Escherichia coli* CMCC44102 and *Clostridium perfringens* cultured for 24 hours were treated with LL-37 and CRAMP, respectively. Numbers indicates relative H_2S content related to the WT bacteria. The results are expressed as mean ± S.D. n = 3 biological replicates. One-way ANOVA followed by Tukey's post hoc analysis. Source data are provided as a Source Data file.

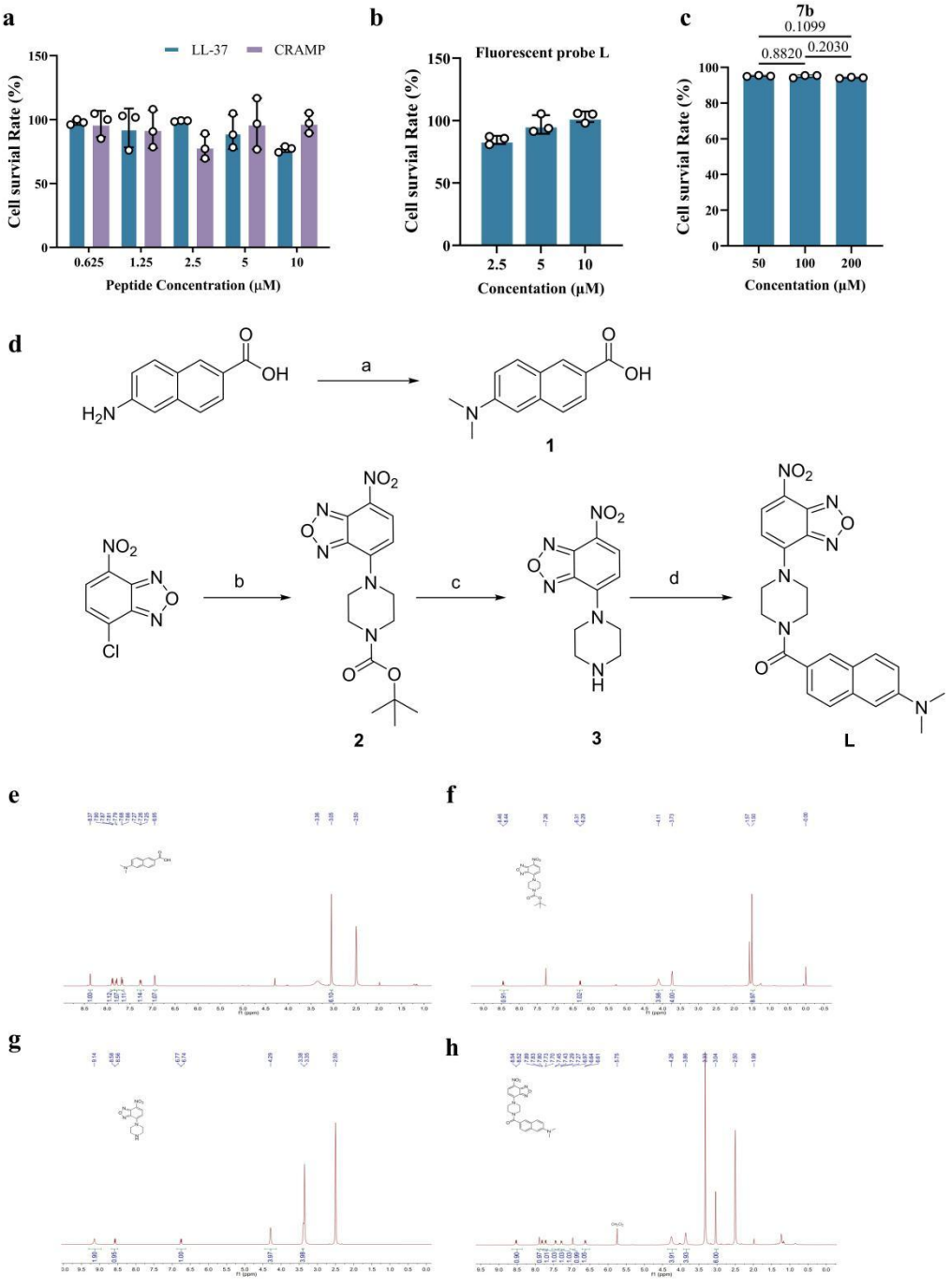

Fig. S4 MTT assay showed the cell viability of RAW264.7 macrophages treated with various concentrations of (**a**) LL-37/CRAMP (0.625, 1.25, 2.5, 5, 10 μM), (**b**) fluorescent probe L (2.5, 5, 10 μM) or (**c**) H_2S scavenger 7b (50, 100, 200 μM) for 24 h. (**d**)Synthesis of the fluorescent H_2S probe L. a) $NaBH_3CN$, HCHO, AcOH, MeOH; b) Tert-butyl piperazine-1-carboxylate, TEA, DCM, reflux; c) TFA/DCM, 0-rt; d) **1**,

HATU, TEA, DCM, rt.The detailed structural elucidation of each compound used in the preparation of fluorescent probe L. (**e**) ^{1}H NMR (400 MHz, DMSO-d_6) of 6-(dimethylamino)-2-naphthoic acid (**1**). (**f**) ^{1}H NMR (400MHz, $CDCl_3$) of tert-butyl 4-(7-nitrobenzo[c][1,2,5]oxadiazol-4-yl)piperazine-1-carboxylate (**2**). (**g**) ^{1}H NMR (400 MHz, DMSO-d_6) of tert-butyl 4-(7-nitrobenzo[c][1,2,5]oxadiazol-4-yl)piperazine-1-carboxylate (**3**). (**h**) ^{1}H NMR (400MHz, $CDCl_3$) of (6-(dimethylamino)naphthalen-2-yl)(4-(7-nitrobenzo[c][1,2,5]oxadiazol-4-yl)piperazin-1-yl)methanone (**4**).The results are expressed as mean ± S.D. n = 3 biological replicates. One-way ANOVA followed by Tukey's post hoc analysis. Source data are provided as a Source Data file.

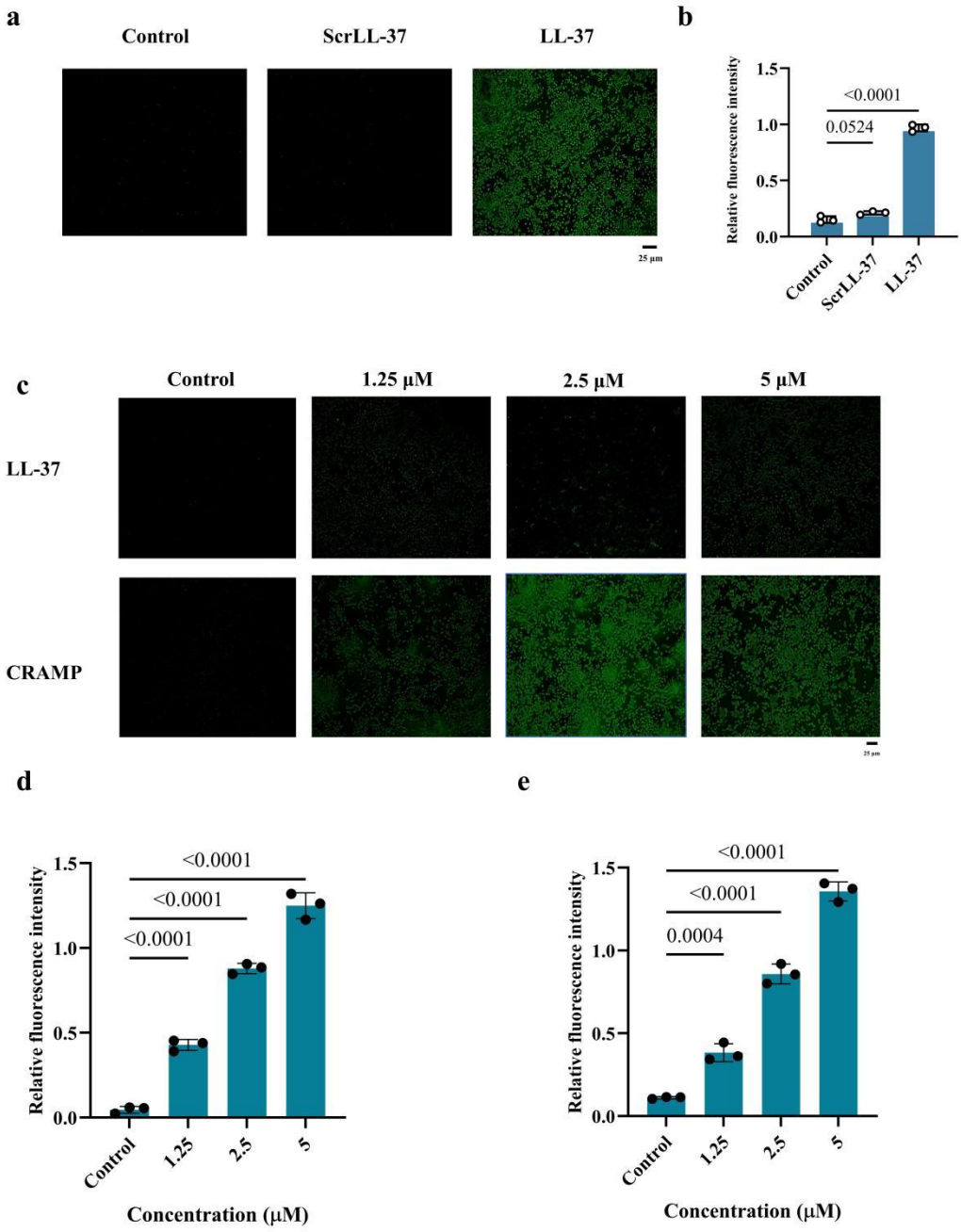

Fig. S5 Extracellular H_2S level was assessed and visualized by a fluorescent H_2S probe under a fluorescent microscope (**a**) and the corresponding quantitative analysis (**b**). Scale bar: 25 μm. Representative images from three independent experiments with similar results. Intracellular H_2S levels were assessed and visualized using the fluorescent H_2S probe WSP-1 under a fluorescent microscope (**c**) and the corresponding quantitative analysis (**d-e**). Scale bar: 25 μm. Representative images from three independent experiments with similar results. The results are expressed as mean ± S.D. n = 3 biological replicates. One-way ANOVA followed by Tukey's post hoc analysis. Source data are provided as a Source Data file.

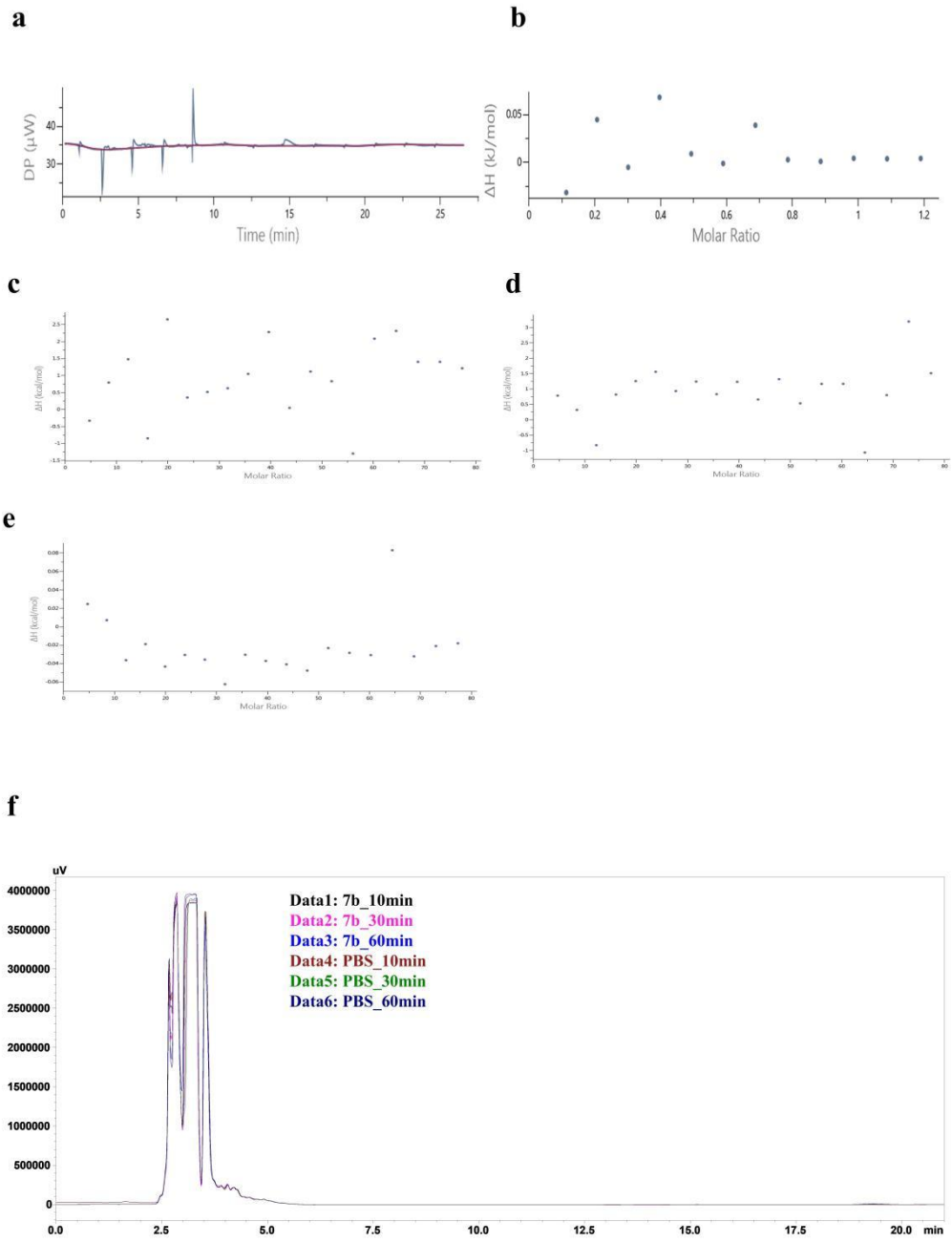

Fig. S6 (**a-b**) The interaction between LL-37 and 7b determined by ITC assay, where 0.5 mM 7b was titrated into 0.05 mM LL-37 in HEPES buffer at 25°C. (**c-e**) The interaction between LL-37 and 7b determined by ITC assay, where 7b was titrated into LL-37 with various concentrations in HEPES buffer at 15°C, 25°C, 37°C. (**f**) High-performance liquid chromatography (HPLC) chromatograms of lysates from *Escherichia coli* CMCC44102 incubated with or without 7b for 10, 30, and 60 min at wavelength of 254 nm.

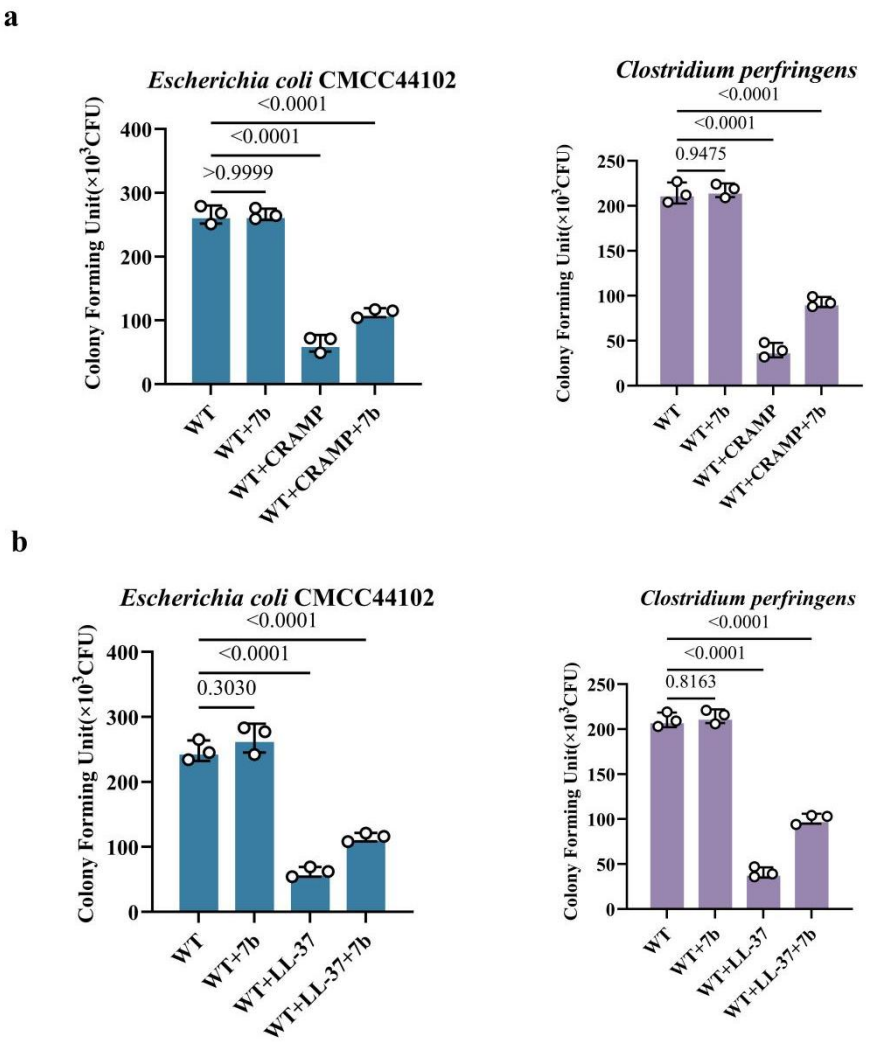

Fig. S7 Colony-forming units (CFUs) counting of *Clostridium perfringens* and *Escherichia coli* CMCC44102 in the presence of CRAMP (**a**) and LL-37 (**b**) with different treatments after 12h incubation. WT: wild-type. The results are expressed as mean ± S.D. n = 3 biological replicates. One-way ANOVA followed by Tukey's post hoc analysis. Source data are provided as a Source Data file.

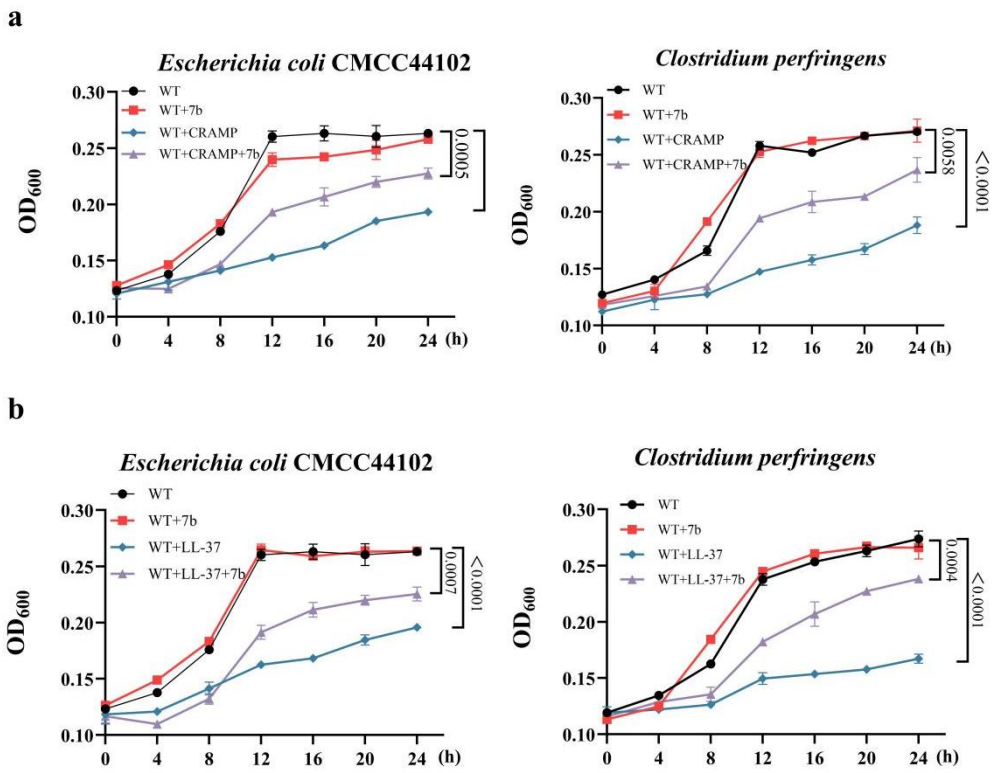

Fig. S8 Representative growth curves of *Escherichia coli* CMCC44102 and *Clostridium perfringens* (1×10^8 CFU/mL) in the presence of CRAMP (**a**) and LL-37 (**b**) (0.5×MIC) in 24 h. Data are expressed as the mean values of optical density at a wavelength of 600 nm (OD_{600}). The results are expressed as mean ± S.D. n = 3 biological replicates. One-way ANOVA followed by Tukey's post hoc analysis. Source data are provided as a Source Data file.

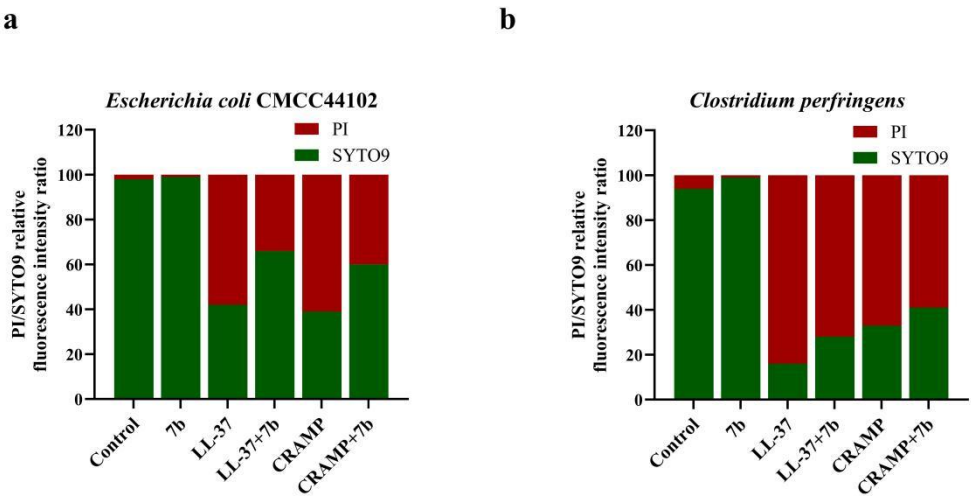

Fig. S9 The relative fluorescence intensities of the two fluorescence signals, PI and SYTO9, in confocal images of (**a**) *Escherichia coli* CMCC44102 and (**b**) *Clostridium perfringens* with treatments of LL-37/CRAMP or in combination of 7b were quantified by imageJ software. Source data are provided as a Source Data file.

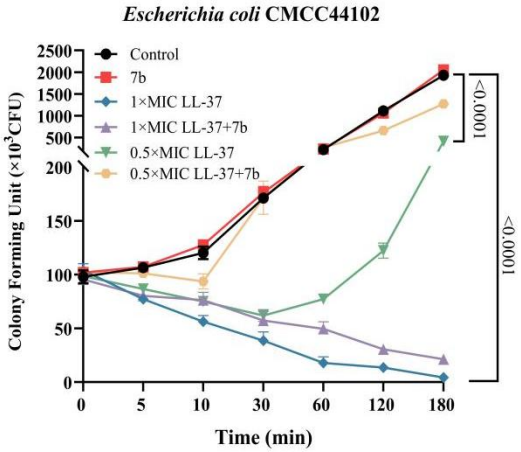

Fig. S10 Growth curves of LL-37 (1×MIC, 0.5×MIC) against *Escherichia coli* CMCC44102 (1×10^5 CFU/mL) with or without 7b co-treatment. The results are expressed as mean ± S.D. n = 3 biological replicates. One-way ANOVA followed by Tukey's post hoc analysis. Source data are provided as a Source Data file.

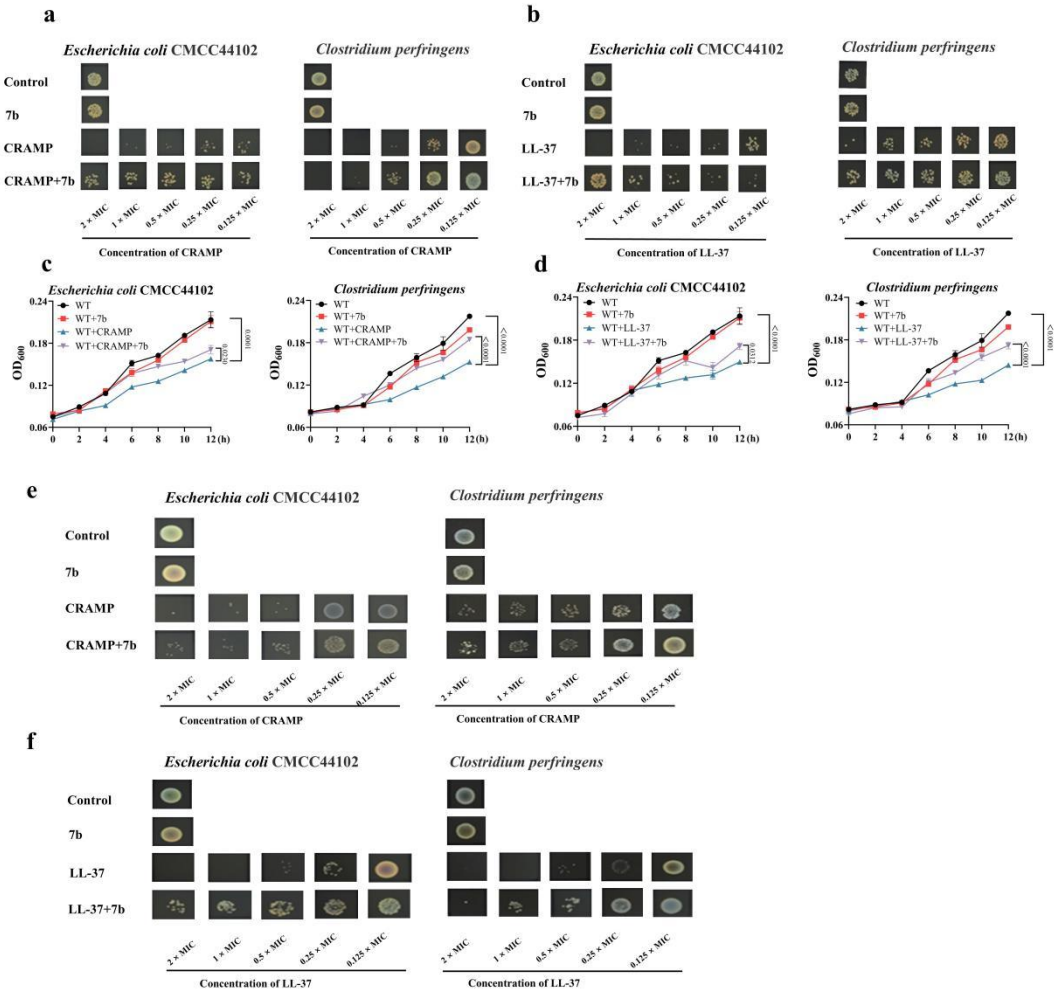

g

Bacteria	Peptides			
	CRAMP		LL-37	
	(μM)	(μg/mL)	(μM)	(μg/mL)
H_2S producing bacteria				
Enterococcus faecalis ATCC29212	38.7	150.0	33.4	150.0
Vibrio alginolyticus	19.4	75.0	16.7	75.0
Non-H_2S producing bacteria				
Staphylococcus aureus	77.4	300.0	66.8	300.0
Methicillinresistant Staphylococcus aureus	77.4	300.0	66.8	300.0
Acinetobacter baumannii 19606	77.4	300.0	66.8	300.0
Pseudomonas aeruginosa CMCC10104	77.4	300.0	66.8	300.0

h

Bacteria	Peptides			
	CRAMP		LL-37	
	(μM)	(μg/mL)	(μM)	(μg/mL)
H_2S producing bacteria				
Enterococcus faecalis ATCC29212	77.4	300.0	66.8	300.0
Vibrio alginolyticus	38.7	150.0	33.4	150.0
Non-H_2S producing bacteria				
Staphylococcus aureus	ND	ND	ND	ND
Methicillinresistant Staphylococcus aureus	ND	ND	ND	ND
Acinetobacter baumannii 19606	ND	ND	ND	ND
Pseudomonas aeruginosa CMCC10104	ND	ND	ND	ND

Fig. S11 H_2S plays a dominant role in the antibacterial activity of LL-37/CRAMP. (**a-b**) Effect of CRAMP and LL-37 on colony formation efficiencies of *Escherichia coli* CMCC44102 and *Clostridium perfringens* in MH without L-cysteine. (**c-d**) Representative growth curves of *Escherichia coli* CMCC44102 and *Clostridium perfringens* in MH without L-cysteine in the presence of CRAMP and LL-37. Data are expressed as the mean values of optical density at a wavelength of 600 nm (OD_{600}). WT: wild-type. (**e-f**) Efficiencies of colony formation of *Escherichia coli* CMCC44102 and *Clostridium perfringens* cultured for 24 hours in the presence of (**e**) CRAMP and (**f**) LL-37.(**g-h**) The minimum inhibitory concentrations (MICs) and minimum bactericidal

concentrations (MBCs) of LL-37/CRAMP against two H_2S-producing and four non-H_2S-producing bacteria. ND means “None detected at the concentration of 300 μg/mL”. The results are expressed as mean ± S.D. n = 3 biological replicates. One-way ANOVA followed by Tukey’s post hoc analysis. Source data are provided as a Source Data file.

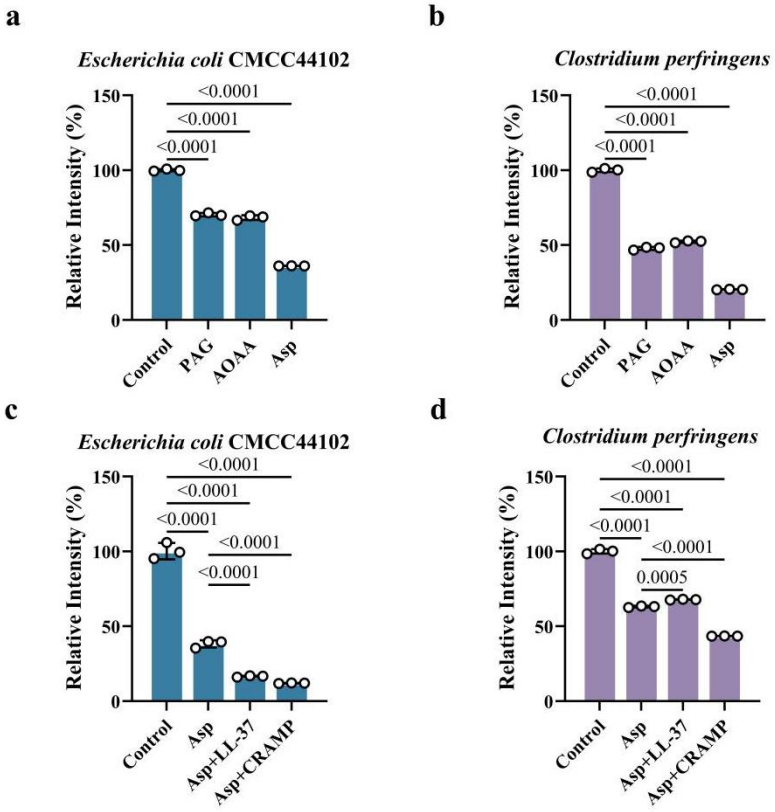

Fig. S12 Quantitative results of brown stains of PbS on representative Pb-acetate–soaked paper strips using imageJ software. Three H_2S-derived enzyme inhibitors (PAG, AOAA, Asp) in (**a**) *Escherichia coli* CMCC44102 and (**b**) *Clostridium perfringens* were screened. Effect of LL-37/CRAMP treatment on H_2S production of (**c**) *Escherichia coli* CMCC44102 and (**d**) *Clostridium perfringens* in the presence of Asp was determined. Numbers indicate relative H_2S content related to the wild-type (WT) bacteria. The results are expressed as mean ± S.D. n = 3 biological replicates. One-way ANOVA followed by Tukey's post hoc analysis. Source data are provided as a Source Data file.

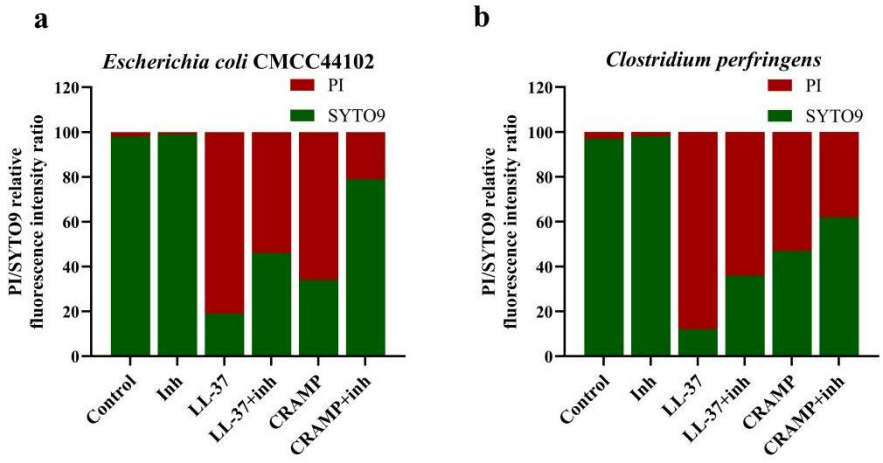

Fig. S13 The relative fluorescence intensities of the two fluorescence signals, PI and SYTO9, in confocal images of (**a**) *Escherichia coli* CMCC44102 and (**b**) *Clostridium perfringens* with treatments of LL-37/CRAMP or in combination of inhibitor were quantified by imageJ software, respectively. Source data are provided as a Source Data file.

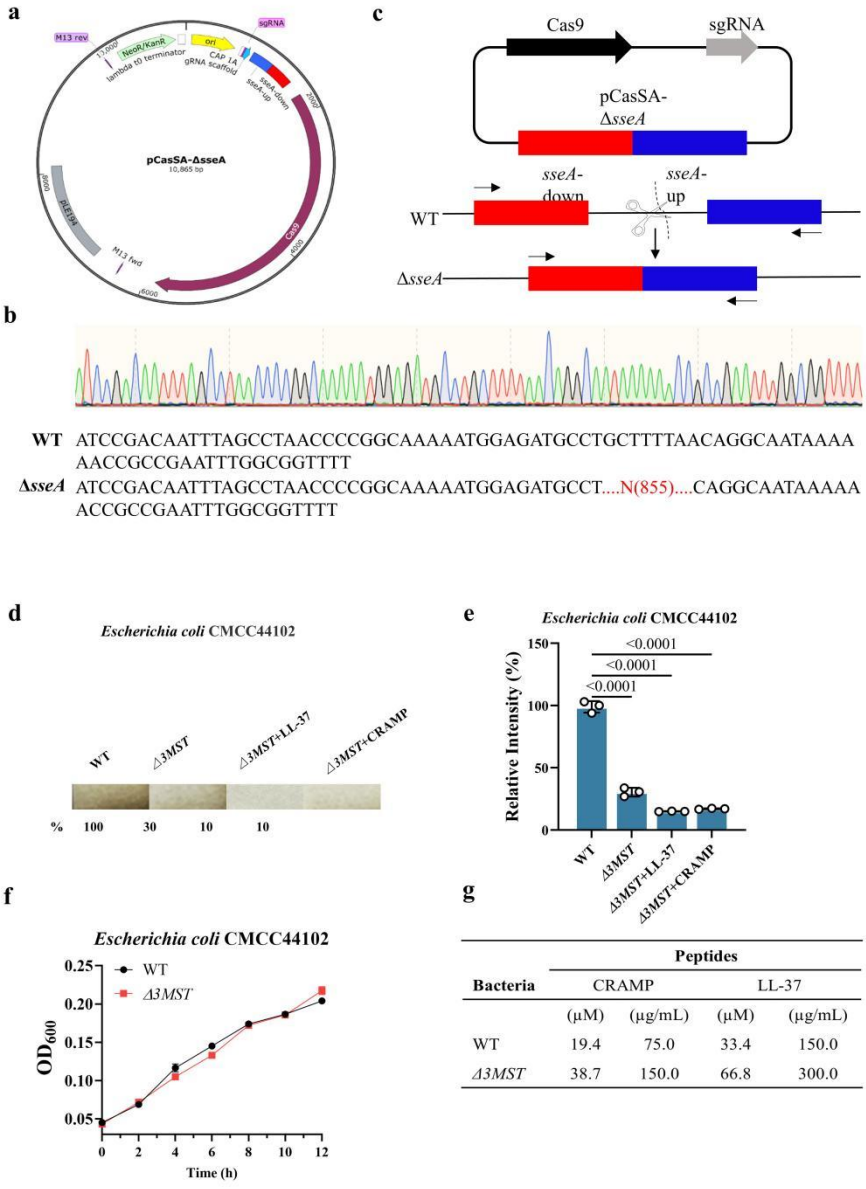

Fig. S14 (**a**) Plasmid construction map of *E. coli* CMCC44102 *sseA* gene knockout strain. (**b**) Comparison of base sequences of Wild-type *E. coli* CMCC44102 (wild-type, WT) and knockout bacteria (Δ*sseA*). (**c**) Schematic diagram of the construction process of *E. coli* CMCC44102 *sseA* gene knockout strain.(**d**) Representative lead acetate dip strips showing brown PbS staining and quantitative values (bottom), wild-type *E. coli* CMCC44102 (wild-type,WT), *E. coli* CMCC44102 *sseA* knockout strain (*Δ3MST*), and LL-37/CRAMP treated *Δ3MST*. (**e**) Quantitation of PbS brown staining on representative lead-acetate soaked strips of *Δ3MST* treated with WT, *Δ3MST* and LL-37/CRAMP using ImageJ software. The number represents the H_2S content relative to WT. (**f**) Representative growth curves of WT and *Δ3MST*. The data point is the average optical density (OD) at a wavelength of 600 nm. (**g**) Minimum inhibitory concentrations (MIC) of LL-37 and CRAMP against WT and *Δ3MST*. WT: wild-type. The results are

expressed as mean ± S.D. n = 3 biological replicates. One-way ANOVA followed by Tukey's post hoc analysis. Source data are provided as a Source Data file.

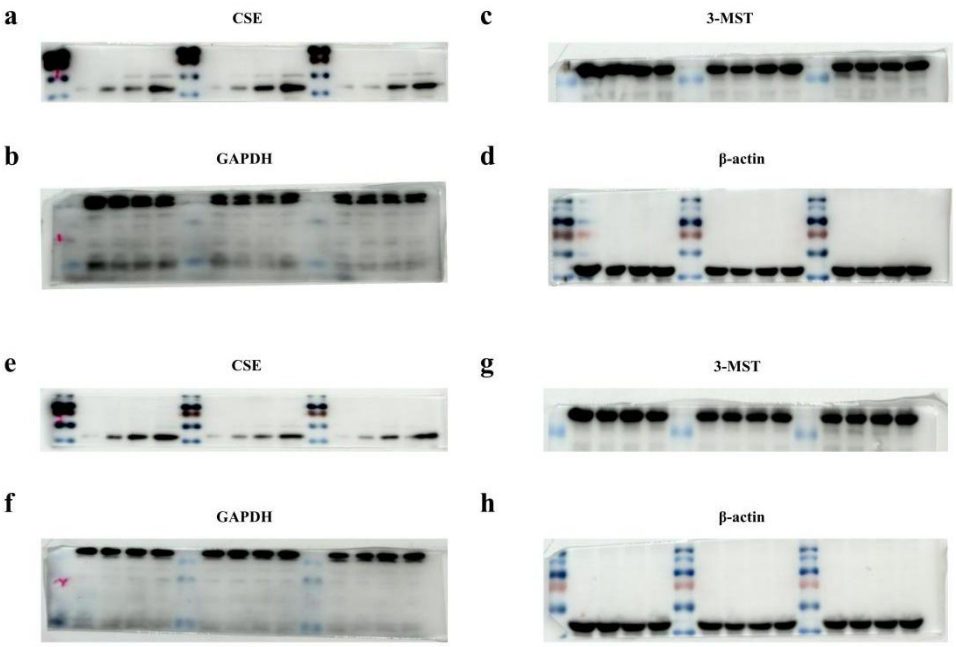

Fig. S15 (**a–b**) Original western blot images showing CSE and GAPDH protein levels in RAW264.7 cells treated with LL-37 (1.25, 2.5, and 5 μM) for 24 h. (**c–d**) Original western blot images showing 3-MST and β-actin protein levels in RAW264.7 cells treated with LL-37 (1.25, 2.5, and 5 μM) for 24 h. (**e–f**) Original western blot images showing CSE and GAPDH protein levels in RAW264.7 cells treated with 5 μM LL-37 for 12, 24, and 36 h. (**g–h**) Original western blot images showing 3-MST and β-actin protein levels in RAW264.7 cells treated with 5 μM LL-37 for 12, 24, and 36 h.

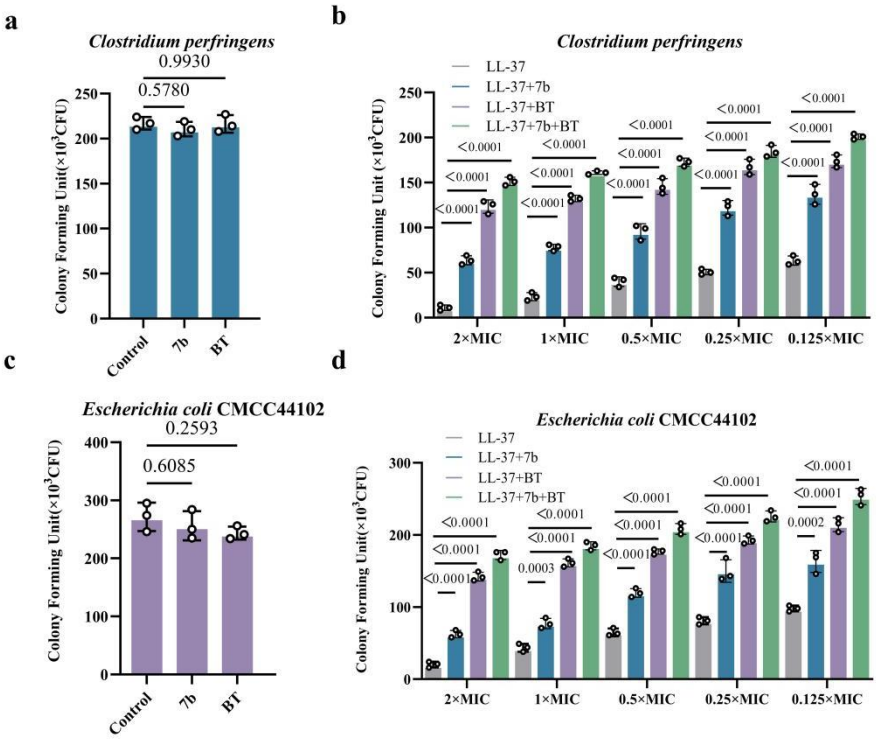

Fig. S16 Colony-forming units (CFUs) counting of (**a-b**) *Clostridium perfringens* and (**c-d**) *Escherichia coli* CMCC44102 (2×10^5 CFU/mL) with different treatments. 7b as H_2S scavengers and bipyridine and thiourea (BT) as ROS scavengers. The results are expressed as mean ± S.D. n = 3 biological replicates. One-way ANOVA followed by Tukey's post hoc analysis. Source data are provided as a Source Data file.

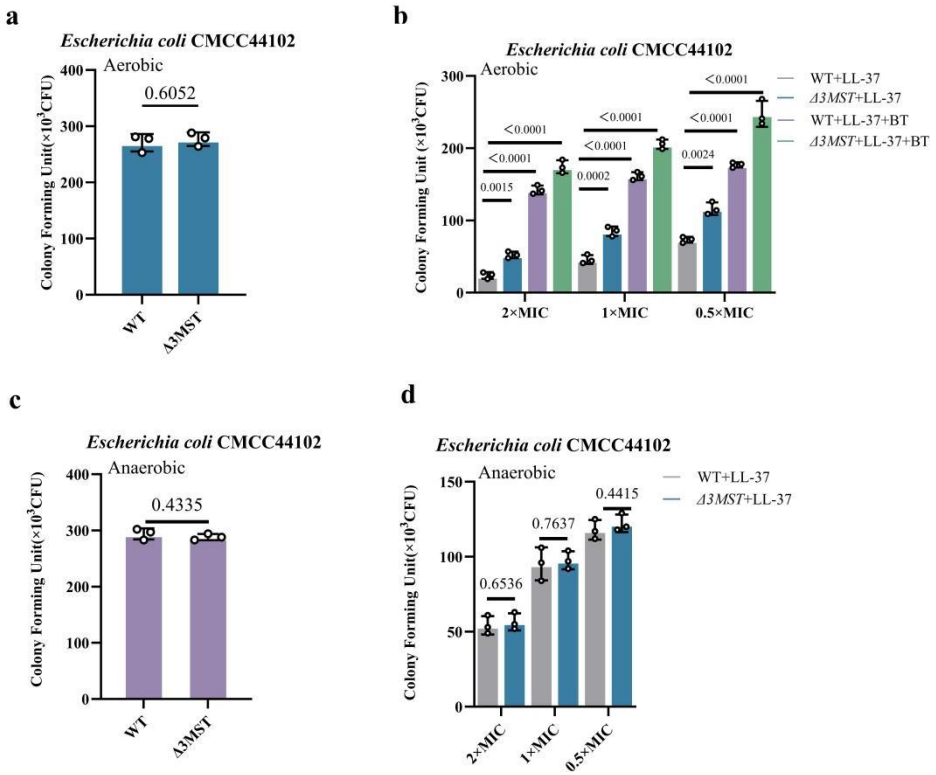

Fig. S17 Colony-forming units (CFUs) counting of the wild-type (WT) and *Δ3MST* (2×10^5 CFU/mL) treated with LL-37 under aerobic (**a-b**) and anaerobic conditions (**c-d**). The results are expressed as mean ± S.D. n = 3 biological replicates. One-way ANOVA followed by Tukey's post hoc analysis. Source data are provided as a Source Data file.

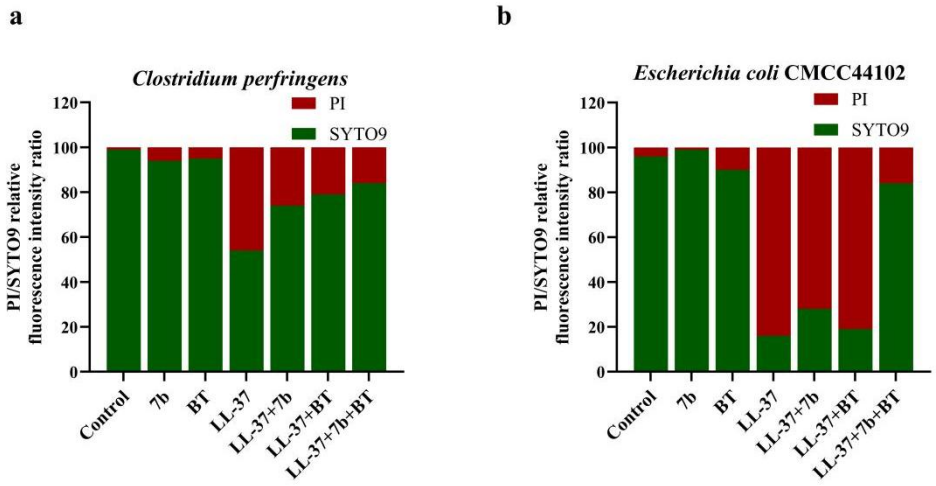

Fig. S18 The relative fluorescence intensities of the two fluorescence signals, PI and SYTO9, in confocal images of (**a**) *Clostridium perfringens* and (**b**) *Escherichia coli* CMCC44102 with different treatments (PBS, 7b, BT, LL-37, LL-37+7b, LL-37+BT, LL-37+7b+BT) were quantified by imageJ software, respectively. Source data are provided as a Source Data file.

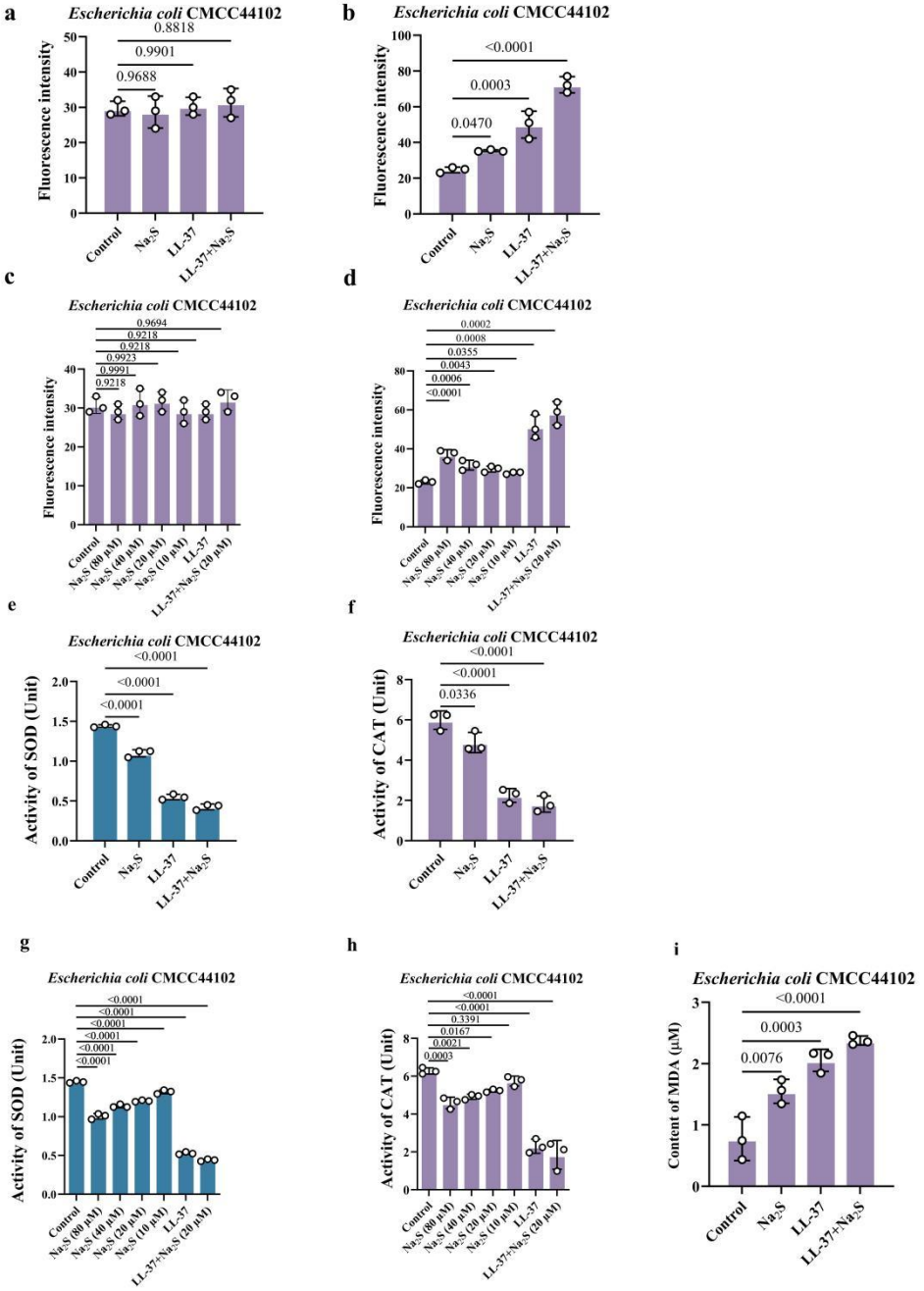

Fig. S19 Effect of Na_2S (100 μM) treatment on the levels of reactive oxygen species (ROS) at 0 h (**a**) and 12 h (**b**) in *Escherichia coli* CMCC44102 (1×10^8 CFU/mL) using DCHF-DA (5 μM) probe at absorbance of 488/525 nm. Effect of Na_2S treatment (80 μM, 40 μM, 20 μM, 10 μM) on the levels of reactive oxygen species (ROS) at 0 h (**c**) and 12 h (**d**) in *Escherichia coli* CMCC44102 (1×10^8 CFU/mL) using DCHF-DA (5 μM) probe at absorbance of 488/525 nm. Effect of Na_2S (100 μM) treatment on the enzymatic activities of superoxide dismutase (SOD) (**e**) and catalase (CAT) (**f**) in *Escherichia coli* CMCC44102 (3×10^7 CFU/mL). Effect of Na_2S treatment (80 μM, 40 μM, 20 μM, 10 μM) on the enzymatic activities of superoxide dismutase (SOD) (**g**) and

catalase (CAT) (**h**) in *Escherichia coli* CMCC44102 (3×10^7 CFU/mL). The results are expressed as mean ± S.D. n = 3 biological replicates. One-way ANOVA followed by Tukey's post hoc analysis. Source data are provided as a Source Data file. (**i**) Effect of Na_2S treatment on malondialdehyde (MDA) content in *Escherichia coli* CMCC44102 (3×10^7 CFU/mL). The results are expressed as mean ± S.D. n = 3 biological replicates. One-way ANOVA followed by Tukey's post hoc analysis. Source data are provided as a Source Data file.

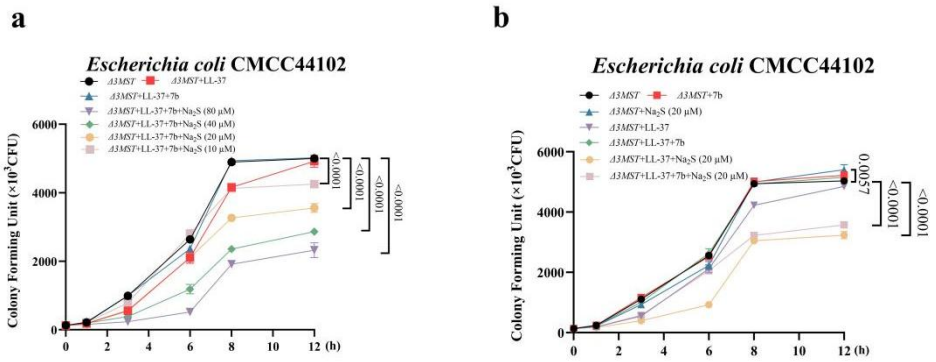

Fig. S20 (**a**) Growth curves of LL-37 (0.5×MIC) in combination with 7b and Na_2S at different concentrations (80, 40, 20, and 10 μM) against the 3MST knockout strain of Escherichia coli CMCC44102. (**b**) Growth curves of LL-37 (0.5×MIC) in combination with 7b and Na_2S (20 μM) against the 3MST knockout strain of Escherichia coli CMCC44102. The results are expressed as mean ± S.D. n = 3 biological replicates. One-way ANOVA followed by Tukey's post hoc analysis. Source data are provided as a Source Data file.

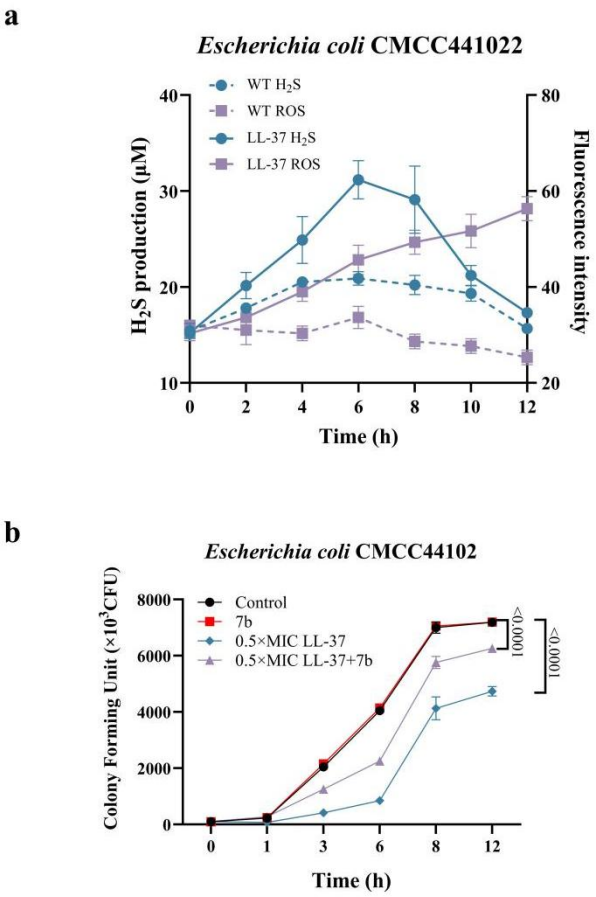

Fig. S21 (**a**) The dynamics of H_2S and ROS levels in *Escherichia coli* CMCC44102 (1×10^8 CFU/mL) before and after treatment with LL-37 (0.5× MIC) over a 12-hour period. WT: wild-type. (**b**) Growth curves of LL-37 (0.5×MIC) against *Escherichia coli* CMCC44102 (1×10^5 CFU/mL) with or without 7b co-treatment. The results are expressed as mean ± S.D. n = 3 biological replicates. One-way ANOVA followed by Tukey's post hoc analysis. Source data are provided as a Source Data file.

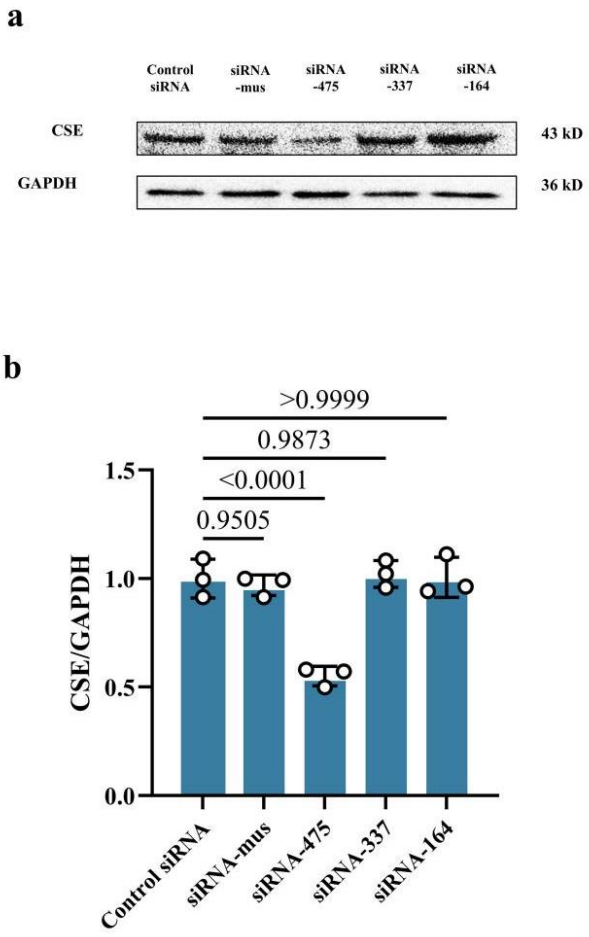

Fig. S22 Suppression of CSE reduced H_2S generation in RAW264.7 macrophages. Screening of CSE proteins by transfection of different siRNA in RAW264.7 macrophages compared with control siRNA. The knockdown efficiency was determined by western blot analysis at 24 h after transfection. GAPDH protein was used as loading controls. The results are expressed as mean ± S.D. n = 3 biological replicates. One-way ANOVA followed by Tukey's post hoc analysis. Source data are provided as a Source Data file.

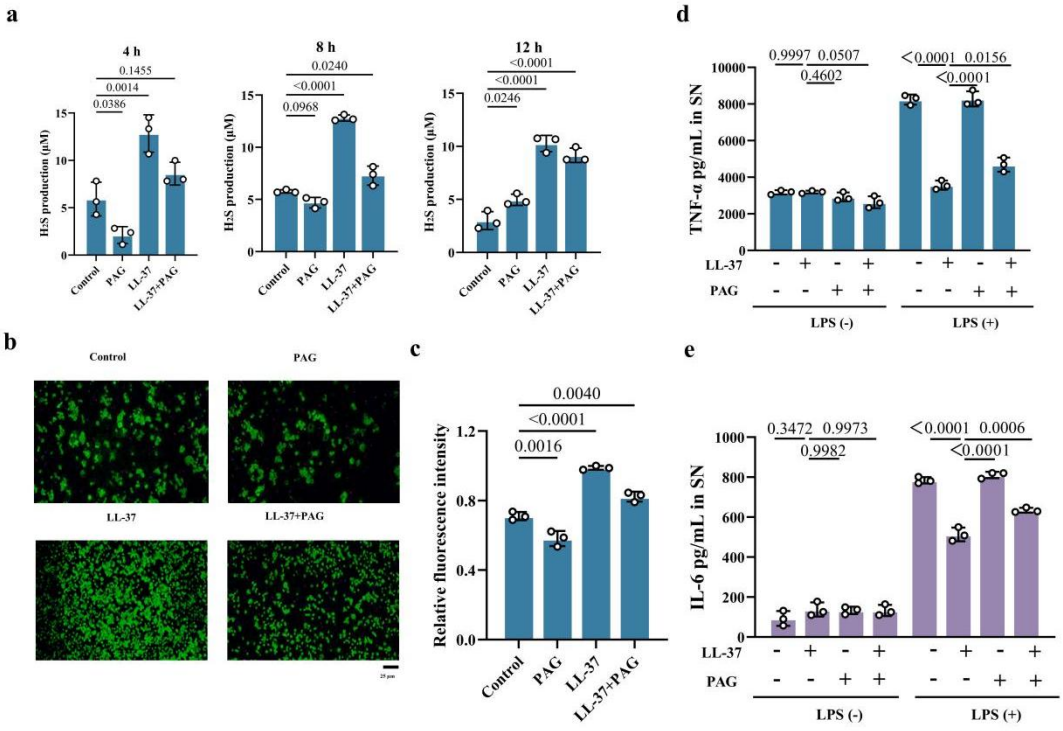

Fig. S23 Inhibitors were introduced to verify H_2S generating enzyme in RAW264.7 macrophages. The H_2S production was indicated by extracellular sulfide level as determined by modified methylene blue method. (**a**) LL-37 promoted H_2S production in RAW264.7 macrophages at 4, 8, and 12 h monitoring times. (**b-c**) Extracellular H_2S level was assessed and visualized by a fluorescent H_2S probe under a fluorescent microscope and the corresponding quantitative analysis. Scale bar: 25 μm. Representative images from three independent experiments with similar results. (**d-e**) TNF-α and IL-6 levels in RAW264.7 macrophages supernatants are detected by ELISA. Cells were pre-treated with or without PAG (1 mM) for 1 h, followed by 100 ng/mL LPS stimulation in the presence or absence of 5 mM LL-37/CRAMP co-treatment for 24 h. The results are expressed as mean ± S.D. n = 3 biological replicates. One-way ANOVA followed by Tukey's post hoc analysis. Source data are provided as a Source Data file.

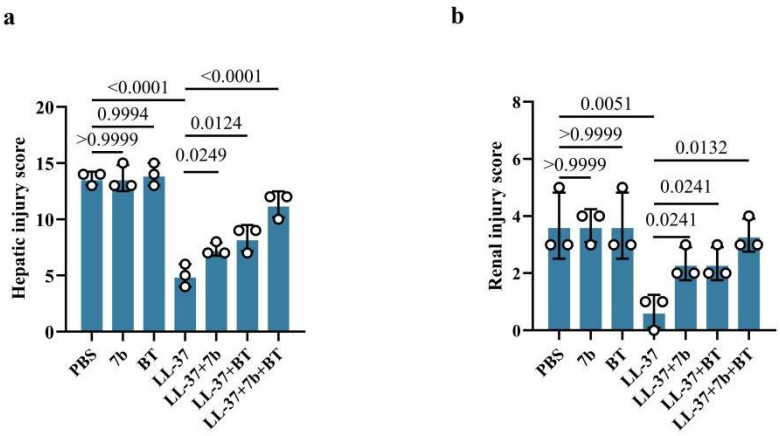

Fig. S24 H&E staining results of liver and kidney. (**a**) Liver injury score and (**b**) kidney injury score after infection in peritonitis mouse with different administration therapy. The results are expressed as mean ± S.D. n = 3 biological replicates. One-way ANOVA followed by Tukey's post hoc analysis. Source data are provided as a Source Data file.

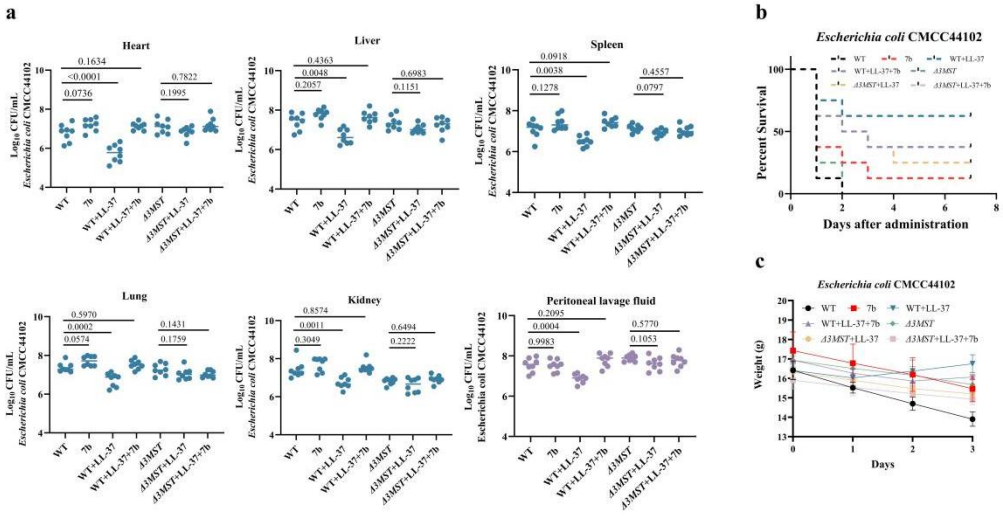

Fig. S25 (**a**) Bacterial burden in heart, liver, spleen, lung, kidney and peritoneal lavage fluid of peritonitis mouse with administration with LL-37 (10 mg/kg), 7b (60 mg/kg) 2 h after intraperitoneal injection of the wild-type (WT) and *Δ3MST Escherichia coli* CMCC44102 (5×10^7 CFU). (**b-c**) Survival and weight changes of mice in different administration groups after intraperitoneal injection of the wild-type (WT) and *Δ3MST Escherichia coli* CMCC44102. The results are expressed as mean ± S.D. n = 8 biological replicates. One-way ANOVA followed by Tukey's post hoc analysis. Source data are provided as a Source Data file.

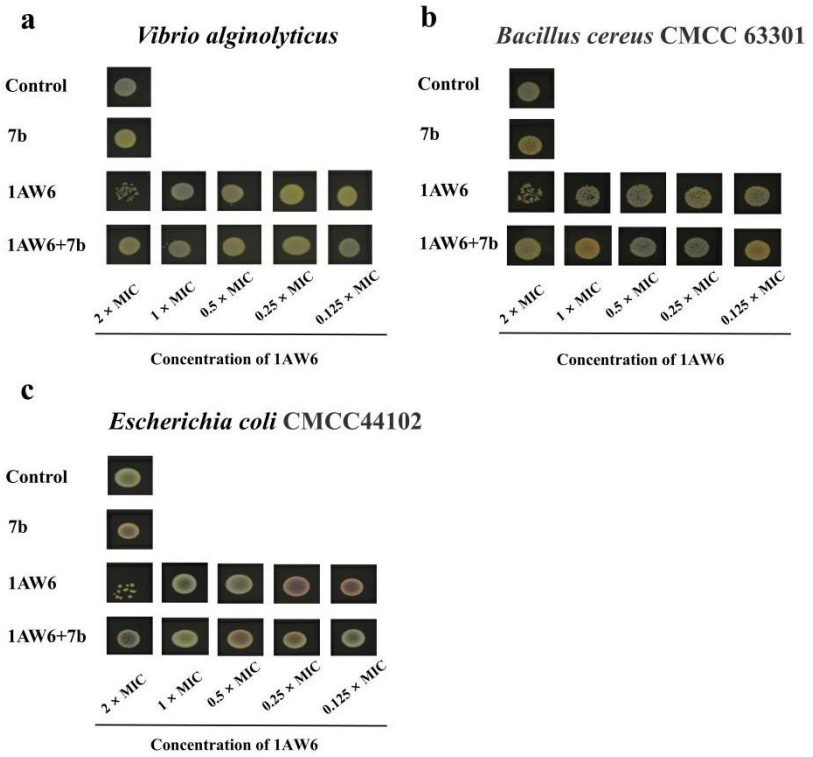

Fig. S26 H_2S acts dominant role in promoting effect in AMP-mediated bacteria killing. Efficiencies of colony formation of (**a**) *Vibrio alginolyticus*, (**b**) *Bacillus cereus* CMCC63301 and (**c**) *Escherichia coli* CMCC44102 in the presence of brevinin-1AW6.

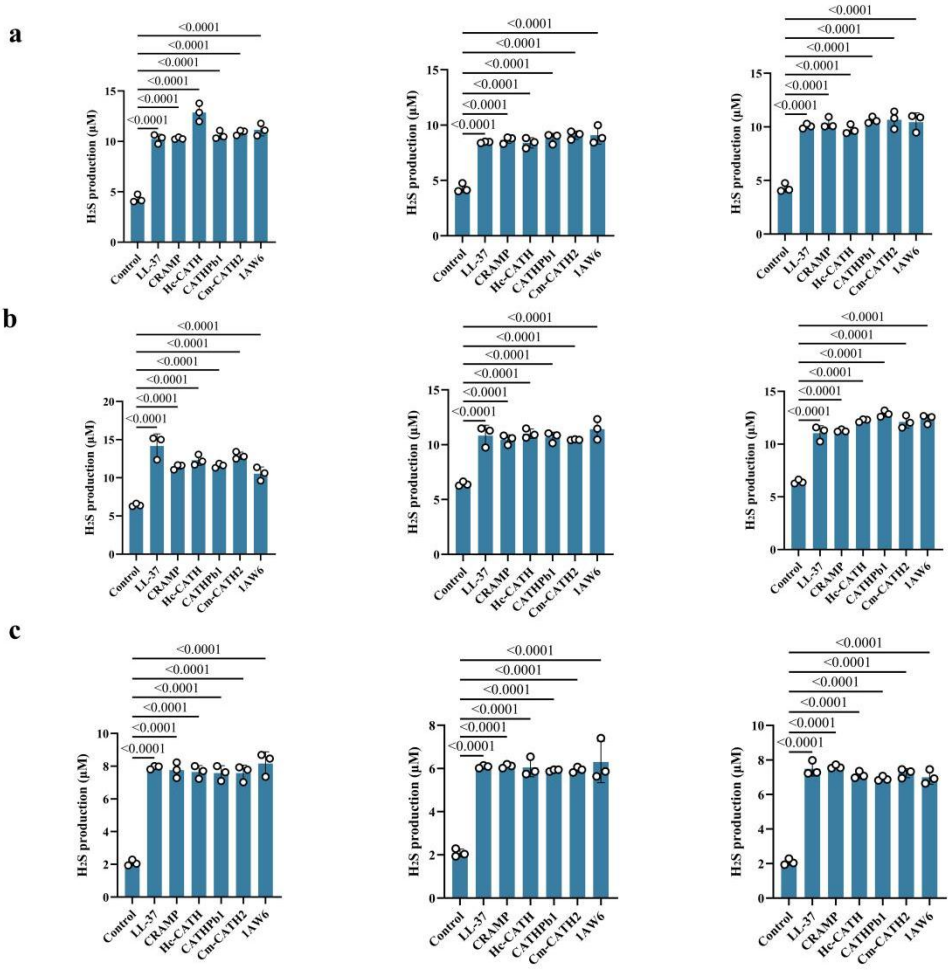

Fig. S27 The results of H_2S production in RAW264.7 macrophages promoted by various concentrations of LL-37, CRAMP, brevinin-1AW6, CATHPb1, Hc-CATH, Cm-CATH2 (1.25, 2.5, 5 μM) under the monitoring time of 8 h (**a**), 12 h (**b**), 24 h (**c**). The results are expressed as mean ± S.D. n = 3 biological replicates. One-way ANOVA followed by Tukey's post hoc analysis. Source data are provided as a Source Data file.

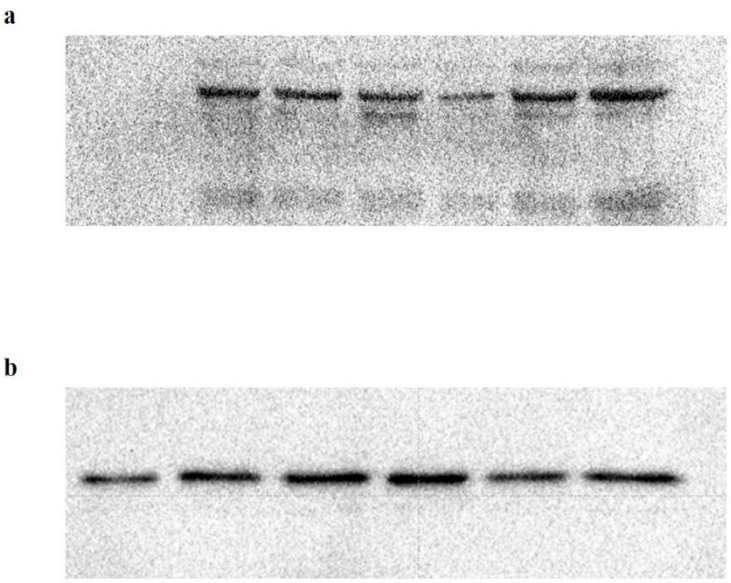

Fig. S28 Original Western blot images corresponding to Fig. S22: (a) CSE protein and (b) GAPDH protein.